



Since January 2020 Elsevier has created a COVID-19 resource centre with free information in English and Mandarin on the novel coronavirus COVID-19. The COVID-19 resource centre is hosted on Elsevier Connect, the company's public news and information website.

Elsevier hereby grants permission to make all its COVID-19-related research that is available on the COVID-19 resource centre - including this research content - immediately available in PubMed Central and other publicly funded repositories, such as the WHO COVID database with rights for unrestricted research re-use and analyses in any form or by any means with acknowledgement of the original source. These permissions are granted for free by Elsevier for as long as the COVID-19 resource centre remains active.



## Investigation of COVID-19-related lockdowns on the air pollution changes in augsburg in 2020, Germany

Xin Cao<sup>a,b</sup>, Xiansheng Liu<sup>c,d,\*</sup>, Hadiatullah Hadiatullah<sup>e,\*\*</sup>, Yanning Xu<sup>f</sup>, Xun Zhang<sup>g</sup>, Josef Cyrus<sup>h</sup>, Ralf Zimmermann<sup>b,i</sup>, Thomas Adam<sup>b,c</sup>

<sup>a</sup> School of Sport Science, Beijing Sport University, Beijing, 100084, China

<sup>b</sup> Joint Mass Spectrometry Center, Cooperation Group Comprehensive Molecular Analytics, Helmholtz Zentrum München, German Research Center for Environmental Health, Ingolstädter Landstr. 1, Neuherberg, 85764, Germany

<sup>c</sup> University of the Bundeswehr Munich, Faculty for Mechanical Engineering, Institute of Chemical and Environmental Engineering, 85577 Neubiberg, Germany

<sup>d</sup> Institute of Environmental Assessment and Water Research (IDAEA-CSIC), 08034, Barcelona, Spain

<sup>e</sup> School of Pharmaceutical Science and Technology, Tianjin University, Tianjin, 300072, China

<sup>f</sup> School of Environmental and Municipal Engineering, Qingdao University of Technology, Qingdao, 266525, China

<sup>g</sup> Beijing Key Laboratory of Big Data Technology for Food Safety, School of Computer Science and Engineering, Beijing Technology and Business University, Beijing, 100048, China

<sup>h</sup> Research Unit Analytical BioGeoChemistry, German Research Center for Environmental Health, Ingolstädter Landstr. 1, 85764 Neuherberg, Germany

<sup>i</sup> Joint Mass Spectrometry Center, Chair of Analytical Chemistry, University of Rostock, Rostock, 18059, Germany

### ARTICLE INFO

#### Keywords:

COVID-19  
Lockdown  
Air pollution  
Random forest  
Traffic volume

### ABSTRACT

The COVID-19 pandemic in Germany in 2020 brought many regulations to impede its transmission such as lockdown. Hence, in this study, we compared the annual air pollutants (CO, NO, NO<sub>2</sub>, O<sub>3</sub>, PM<sub>10</sub>, PM<sub>2.5</sub>, and BC) in Augsburg in 2020 to the record data in 2010–2019. The annual air pollutants in 2020 were significantly ( $p < 0.001$ ) lower than that in 2010–2019 except O<sub>3</sub>, which was significantly ( $p = 0.02$ ) higher than that in 2010–2019. In a depth perspective, we explored how lockdown impacted air pollutants in Augsburg. We simulated air pollutants based on the meteorological data, traffic density, and weekday and weekend/holiday by using four different models (i.e. Random Forest, K-nearest Neighbors, Linear Regression, and Lasso Regression). According to the best fitting effects, Random Forest was used to predict air pollutants during two lockdown periods (16/03/2020–19/04/2020, 1st lockdown and 02/11/2020–31/12/2020, 2nd lockdown) to explore how lockdown measures impacted air pollutants. Compared to the predicted values, the measured CO, NO<sub>2</sub>, and BC significantly reduced 18.21%, 21.75%, and 48.92% in the 1st lockdown as well as 7.67%, 32.28%, and 79.08% in the 2nd lockdown. It could be owing to the reduction of traffic and industrial activities. O<sub>3</sub> significantly increased 15.62% in the 1st lockdown but decreased 40.39% in the 2nd lockdown, which may have relations with the fluctuations the NO titration effect and photochemistry effect. PM<sub>10</sub> and PM<sub>2.5</sub> were significantly increased 18.23% and 10.06% in the 1st lockdown but reduced 34.37% and 30.62% in the 2nd lockdown, which could be owing to their complex generation mechanisms.

### 1. Introduction

Air pollution has been one of the major problems in the whole world, which severely threatens human health (Kim et al., 2013). According to World Health Organization (WHO), every year more than 7 million

deaths are attributed to air pollutants (<https://www.who.int/westernpacific/health-topics/air-pollution>). For example, particulate matters (PMs), which refer to tiny particles in the air adsorbing polycyclic aromatic hydrocarbons (PAHs), heavy metals, and other volatile organic fragments, can be breathed into human lungs leading to pulmonary

Peer review under responsibility of Turkish National Committee for Air Pollution Research and Control.

\* Corresponding author. University of the Bundeswehr Munich, Faculty for Mechanical Engineering, Institute of Chemical and Environmental Engineering, 85577 Neubiberg, Germany.

\*\* Corresponding author.

E-mail addresses: [xianshengnj@126.com](mailto:xianshengnj@126.com) (X. Liu), [hadi66@tju.edu.cn](mailto:hadi66@tju.edu.cn) (H. Hadiatullah).

<https://doi.org/10.1016/j.apr.2022.101536>

Received 29 June 2022; Received in revised form 15 August 2022; Accepted 15 August 2022

Available online 21 August 2022

1309-1042/© 2022 Turkish National Committee for Air Pollution Research and Control. Production and hosting by Elsevier B.V. All rights reserved.

diseases (Araujo, 2011) and enter blood circulation to induce cardiovascular diseases (Lawal, 2017). Black carbon (BC) belongs to PMs and is generated from incomplete combustion (Liu et al., 2021a), which showed potential carcinogenic effects on human (Arif and Parveen, 2021). O<sub>3</sub> is a very reactive and oxidative pollutant, which can damage the human skin, eyes, and mucosae (World Health Organization, 2003) as well as cause inflammation in bronchia leading to respiratory diseases (Kim et al., 2020; Szyszkowicz and Rowe, 2016). CO is toxic and easy to combine with hemoglobin, which can block the transmission of oxygen. A high level of CO can cause human dizziness and even death (<https://www.epa.gov/co-pollution>). Until now, the study about air pollution on human health has attracted wide attentions.

In the early 2020, coronavirus (COVID-19) appeared in most of the countries and caused huge casualties and deaths (Hu et al., 2021), which was firstly reported in November 2019 in Wuhan, China. COVID-19 is a kind of coronavirus which spreads by small droplets and particles exhaled by human and causes acute respiratory syndrome (Jayaweera et al., 2020). In order to suppress the spread of COVID-19, many countries used emergency measures to block its transmission, for example, wearing masks, social distance, and lockdown. The traffic density was greatly attenuated and the human activities were largely limited during lockdown (Burns et al., 2021). The emergency rules reduced the activities of human but gave a new perspective to study air pollutants to understand how human activities contribute to it (Kumari and Toshniwal, 2020). For example, Das et al. (2021) showed that the air quality was greatly improved in India urban cities during lockdown. Improvement of air quality during lockdown were also reported in China (Xu et al., 2020), Italy (Gualtieri et al., 2020), Spain (Briz-Redón et al., 2021), Egypt (Abou El-Magd and Zanaty, 2021), and New Zealand (Patel et al., 2020). In Germany, the first COVID-19 case was reported in January 27, 2020. The affected population gradually increased and multiple regulations were implemented (e.g. lockdown). The first national wide lockdown started from March 16, 2020 to the April 19, 2020 (1st lockdown). And the second national wide lockdown started from November 02, 2020 to December 31, 2020 (2nd lockdown).

Although general COVID-related decreases in the concentrations of air pollutants have been shown in major Germany cities (Burns et al., 2021) and around the world (Kumari and Toshniwal, 2020), closer examinations are required to be done on a city-by-city manner. The COVID-related air quality changes investigations were mainly focused on two fields. One aspect was to compare the air quality during anti-COVID measurement implementation to the adjacent periods e.g. pre- or post-lockdown (Das et al., 2021; Collivignarelli et al., 2020; Tobias et al., 2020; Dantas et al., 2020) or to the previous years' records (Xu et al., 2020; Gualtieri et al., 2020; Abou El-Magd and Zanaty, 2021; Patel et al., 2020; Kumari and Toshniwal, 2020). The other aspect was to predict air pollutants based on meteorological parameters and other factors such as minor- or major-lockdown (Briz-Redón et al., 2021; Munir et al., 2021; Wang et al., 2021; Bera et al., 2021) to evaluate the reductions of air pollution, however, in those air pollution simulations, traffic variable was missing since it was a very important factor for air pollutants predictions. In order to accurately predict the air pollutants, traffic factor should be considered in the statistical model simulations. In addition, the evaluation of air quality changes attributed to lockdowns in Augsburg is still not reported.

Therefore, in this study, we are interested to explore how COVID-19 pandemic in 2020 impacted on air pollution in Augsburg as well as how lockdown impacted air pollutants in Augsburg. Hence, we aimed to compare the annual levels of seven air pollutants (CO, NO, NO<sub>2</sub>, O<sub>3</sub>, PM<sub>10</sub>, PM<sub>2.5</sub>, and BC) in Augsburg between 2010 and 2019 and 2020; then we built the different models (i.e. Random Forest, K-nearest Neighbors, Linear Regression, and Lasso Regression) based on meteorological parameters, traffic factor, and human activities variables (weekday/weekend/holiday) to simulate and predict the different air pollutants in 2020 assuming the lockdown was not implemented; finally, we found the Random Forest showed the best fitting effects to predict air

pollutants in Augsburg and clarified how lockdown impacted on air pollutants. In general, the larger data is still required to better investigate the impact of lockdown on reduction on air pollutant.

## 2. Methodology

### 2.1. Geographical study area

Augsburg is the third largest city and an important traffic junction in Bavaria, Germany with 300,000 inhabitants in its metropolitan area. Two rivers (Wertach and Lech) flow through the city. It has a semi-continental climate with cold winter and warm summer, which sea level is above 500 m with the annual temperature of 13.2 °C, annual precipitation of 750 mm, and annual sunshine duration of 1750 h. The fixed air pollutants monitoring stations (Fig. 1 for detecting CO, NO, NO<sub>2</sub>, O<sub>3</sub>, PM<sub>2.5</sub>, and PM<sub>10</sub>) in Augsburg are at Bourges-Platz (48.36° N, 10.91° E, located in a park between two streets since 1986 regarded as urban background), Karlstraße (48.37° N, 10.90° E, located at a four-lane with high traffic volume since 2003 regarded as urban traffic), Königsplatz (48.36° N, 10.90° E, located in a strip between two streets since 1975 regarded as urban traffic), and Bayerisches Landesamt für Umwelt (48.32° N, 10.90° E, located at Bavarian state office for the environment since 2000 regarded as suburban background). Meanwhile, the monitor station (Fig. 1 for detecting BC) was operated jointly since 2004 by Helmholtz Zentrum München (German Research Center for Environmental Health, Munich) and Environmental Science Center, Augsburg University to monitor the air pollution at the site of University of Applied Science (UAS, 48.36° N, 10.91° E) (Pitz et al., 2008). Traffic monitoring stations are distributed in Augsburg on the main roads and the typical sites are shown in Fig. 1. Traffic density was counted in each monitoring station for every 15 min interval in each direction. We summed up four intervals to get the hourly traffic density data.

### 2.2. Data collection

The hourly data of CO, NO, NO<sub>2</sub>, O<sub>3</sub>, PM<sub>2.5</sub>, and PM<sub>10</sub> concentrations (01/01/2010–31/12/2020) were obtained from the Federal Environment Agency (UBA) (<https://www.umweltbundesamt.de/en/>) by real-time fixed air pollutants monitoring stations distributed in the cities. The hourly data of BC concentrations (01/01/2018–31/12/2020) were obtained from the site of UAS. Then, the annual air pollutants in 2020 to that in 2010–2019 average were compared. The hourly meteorological data in Augsburg (01/08/2016–31/12/2020) were available online from German Weather Service (Deutscher Wetterdienst). The meteorological observations included pressure, temperature, relative humidity, precipitation, wind speed, and wind direction. Hourly traffic density data in Augsburg (01/08/2016–31/12/2020) were accessed from data recorded by the Augsburg city authorities. Weekday and weekend/holiday (01/08/2016–31/12/2020) were categorized according to the local public calendar to distinguish the different human living styles.

### 2.3. Simulation and application of models

In the processes of setting up models, the hourly meteorological and traffic data (01/08/2016–30/09/2019) were used as variables to simulate models. Due to the holiday effect (Adame et al., 2014), pollutant concentrations differed between weekday and holiday (Saturday, Sunday, and holiday). Hence the input factors of weekday and weekend/holiday were differently regarded as 1 and 2, respectively, based on the date in 01/08/2016–30/09/2019 according to the local public calendar. The simulated air pollutants were shown as the following equation.

$$\text{Estimated pollutants} = Y_j \sim X_i \quad (1)$$

where Y<sub>j</sub> represents the concentration of hourly BC, CO, NO, NO<sub>2</sub>, O<sub>3</sub>,

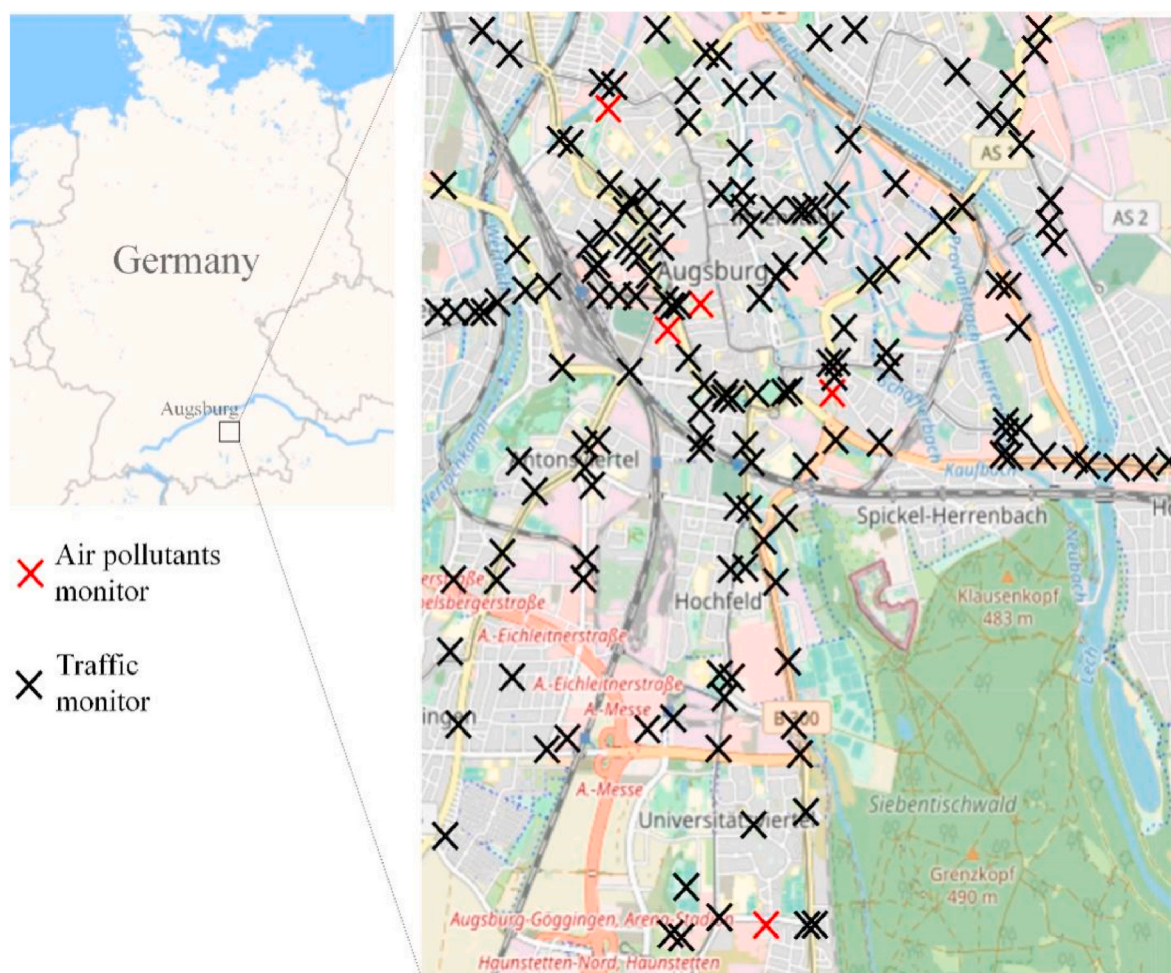


**Fig. 1.** The geographical features of Augsburg and the distributions of air pollutants and traffic monitors in Augsburg.

PM<sub>10</sub>, and PM<sub>2.5</sub>, respectively.  $X_i$  represents the hourly value of pressure, air temperature, relative humidity, precipitation, wind speed, wind direction, weekday/weekend/holiday, and traffic density.

The results of the simulations were operated by Python scripts. We compared four different simulation models, including Random Forest (a supervised and powerful machine learning algorithm based on decision trees, which can be used for both classification and regression) (Gaiazzo et al., 2020), K-nearest Neighbors (the most widely used algorithm for both classification and regression based on the idea that similar things are near together) (Aini and Mustafa, 2020), Linear Regression (the mostly used algorithm to find the relationships between dependent and independent variables) (Yuchi et al., 2019), and Lasso Regression (improved from linear regression using the regularization way to reduce overfit) (Sethi and Mittal, 2021). The dependent variables (air pollutants) and independent variables (meteorological indicators, traffic data, holidays, etc.) (01/08/2016–30/09/2019) were input to each model to simulate pollutant concentrations separately, and the models were compared by the evaluation parameters, i.e. correlation coefficient ( $R^2$ ), the mean squared error (MSE), root mean square error (RMSE), mean absolute error (MAE), and mean absolute percentage error (MAPE).

At the beginning of setting models, the training and testing data splitting proportions were set as 50:50, 70:30, and 90:10 for each model to select the best splitting proportion for machine learning. In order to avoid over-fitting, five-fold cross-validation was used for the establishment of models (Fig. S1). The best fitting model i.e. Random Forest (the detailed hyper-parameters of Random Forest shown in Table S1) was further used to predict air pollution concentrations without lockdown.

The hourly meteorological data in two lockdowns were used for the Random Forest prediction. We assumed the traffic density during two lockdown periods were similar to the corresponding periods in the record date in 16/03–19/04 and 02/11–31/12 (2016–2019), which were used for the prediction.

#### 2.4. Data analysis

The air pollutants data were reported as an average concentration  $\pm$  standard deviation (SD), which significant difference was evaluated by the analysis of variance (ANOVA) using SPSS software (IBM SPSS Statistics 25, Chicago, IL, USA). The Pearson correlations between hourly average of different air pollutants (CO, NO, NO<sub>2</sub>, O<sub>3</sub>, PM<sub>2.5</sub>, PM<sub>10</sub>, and BC) and meteorological data (pressure, temperature, relative humidity, wind speed, and wind direction) as well as traffic data and weekdays and weekends/holidays were calculated (Table S2) by using SPSS software (IBM SPSS Statistics 25, Chicago, IL, USA). Only the data (meteorological data, traffic data, and weekdays and weekends/holidays) with significant ( $p < 0.05$ ) Pearson relationships to the air pollutants were used for the model simulation. Wind flow diagrams presented on radius graphs were made by Origin analysis software based on PM<sub>10</sub>, PM<sub>2.5</sub>, and BC with wind direction and wind speed data.

### 3. Results and discussion

#### 3.1. Annual air pollution during study periods in augsburg

The average of air pollutants was significantly different in different

seasons during 2010–2019. Briefly, the seasonal fluctuations of CO in 2010–2019 (Table S3) were higher in autumn ( $0.37 \pm 0.06 \text{ mg/m}^3$ ) and winter ( $0.45 \pm 0.06 \text{ mg/m}^3$ ) than in spring ( $0.35 \pm 0.06 \text{ mg/m}^3$ ) and summer ( $0.27 \pm 0.01 \text{ mg/m}^3$ ). NO in 2010–2019 (Table S3) were also higher in autumn ( $25.51 \pm 8.66 \text{ }\mu\text{g/m}^3$ ) and winter ( $26.84 \pm 8.23 \text{ }\mu\text{g/m}^3$ ) than that in spring ( $16.54 \pm 5.25 \text{ }\mu\text{g/m}^3$ ) and summer ( $11.45 \pm 1.57 \text{ }\mu\text{g/m}^3$ ). This could be due to the residential heating in winter time (Zhang et al., 2009) and low temperature and precipitation (Li et al., 2017), since the high temperature can promote the volatilization of air pollutants, and rainfall can deposit the air pollutants (Xu et al., 2016). This result was also supported by our meteorological data (Table S4) where the temperature and precipitation in autumn ( $9.44 \pm 6.24 \text{ }^\circ\text{C}$  and  $14.28 \pm 22.96 \text{ mm}$ ) and winter ( $0.65 \pm 4.89 \text{ }^\circ\text{C}$  and  $7.24 \pm 17.82 \text{ mm}$ ) were lower than that in spring ( $9.64 \pm 6.53 \text{ }^\circ\text{C}$  and  $20.32 \pm 25.02 \text{ mm}$ ) and summer ( $18.72 \pm 5.26 \text{ }^\circ\text{C}$  and  $28.02 \pm 25.83 \text{ mm}$ ). The seasonal fluctuations of O<sub>3</sub> in 2010–2019 was higher in spring ( $55.62 \pm 8.55 \text{ }\mu\text{g/m}^3$ ) and summer ( $64.19 \pm 5.87 \text{ }\mu\text{g/m}^3$ ) than that in autumn ( $27.05 \pm 9.95 \text{ }\mu\text{g/m}^3$ ) and winter ( $30.46 \pm 6.37 \text{ }\mu\text{g/m}^3$ ). It attributed to O<sub>3</sub> formation where the volatile organic compounds (VOCs) and NO<sub>x</sub> react to produce O<sub>3</sub> under high temperature and long sunlight (photochemistry) (Balmes et al., 2019).

In comparison, the annual of air pollutants (CO, NO, NO<sub>2</sub>, PM<sub>10</sub>, PM<sub>2.5</sub>, and BC) in 2020 was significantly ( $p < 0.001$ ) lower than that in 2010–2019 (Fig. 2 and Table S5), which indicated that anti-COVID-19 measures during COVID-19 pandemic in 2020 (e.g., limitation of traffic and human activities) greatly reduced CO, NO, NO<sub>2</sub>, PM<sub>10</sub>, PM<sub>2.5</sub>, and BC emissions. While, O<sub>3</sub> was significantly ( $p = 0.02$ ) higher in 2020 than that in 2010–2019, which indicated that O<sub>3</sub> pollution was also affected by those measures. These phenomena were also comparable with previous studies (Balamurugan et al., 2021; Cazoria et al., 2021; Sicard et al., 2020).

### 3.2. The best fitting model and its driving factors

#### 3.2.1. The best fitting model

The splitting proportion of training data and test data were set as 50:50, 70:30, and 90:10 for four models. The fitting effects were compared and summarized in Table 1, based on R<sup>2</sup>, MSE, RMSE, MAE, and MAPE for test data (Table S6). As a result, Random Forest showed the best fitting effects than the other three models for all air pollutants. In addition, Random Forest showed different fitting effects for each air pollutant by using different splitting proportions. Based on the optimized fitting effects, 90:10 was chosen as the best splitting proportion for CO, NO, NO<sub>2</sub>, O<sub>3</sub>, PM<sub>10</sub>, and PM<sub>2.5</sub>, with R<sup>2</sup> of 0.585, 0.526, 0.585, 0.747, 0.559, and 0.613, respectively. While 70:30 splitting proportion was selected for BC with R<sup>2</sup> of 0.452.

#### 3.2.2. Driving factors for each variable

The uneven distributions of air pollutants were influenced by meteorological factors and human activities (e.g., traffic emission, heating activities) (Liu et al., 2021b). Once pollutants were emitted into the atmosphere, their dispersion, transportation, and transformation were largely dependent on related meteorological conditions. However, the effects of meteorological factors on air pollution were typically discussed in qualitative methods (Chen et al., 2008; Wang et al., 2010). Therefore, the quantitative analysis between air pollutants concentrations and meteorological factors was discussed in this section. In Random Forest, driving factor is used to reflect the effect of each variable, which is helpful to recognize the most important variables. In Fig. 3, air temperature and wind speed were the two most important variables which were higher than 0.19 and 0.15 for all air pollutants, respectively. Since low temperature impacts air mass movement and tends to trap air pollutants near the ground (Zhang et al., 2018). Especially, the emission of BC from gasoline and diesel-powered vehicles may increase under low temperatures condition due to incomplete combustion (Krecl et al., 2020). Strong wind is effective to blow out air

pollutants, since the particles are impeded to accumulate (Liu et al., 2021b). Conversely, air pollutants accumulate under low and calm winds (Begam et al., 2016), where indicating the pollution is highly dependent on local emissions (Liu et al., 2020b; Shen et al., 2015). In our study, CO, NO, NO<sub>2</sub>, and BC were lower in the 1st lockdown in 2020 than that in the corresponding period in 2016–2019 (Table S7). All air pollutants in the 2nd lockdown in 2020 were lower than that in 2016–2019. However, the temperature was not significantly different between 2020 and 2016–2019 in two lockdowns. The wind speed only made a significant difference in the 2nd lockdown (higher in 2016–2019 than that in 2020) but not in the 1st lockdown. It indicated that the changes of air pollution were attributed to their combined factors (e.g. temperature, wind speed, and traffic flow). Relative humidity was less than 0.11 for all air pollutants except for O<sub>3</sub> which was as high as 0.42. Although the relative humidity has less impact to PM concentrations, but its fluctuation raised the concentrations of PM (Zhang et al., 2017). In addition, the contributions of traffic to CO, NO, NO<sub>2</sub>, and BC were higher than 0.15, indicating the traffic was an important source for these pollutants which was also supported by reported studies (Dantas et al., 2020; Farias and ApSimon, 2006; Tobias et al., 2020). Our previous study already found that the direct traffic emission could be an important source for BC in Augsburg (Liu et al., 2021c). The traffic flows (Table S8) were greatly decreased both in the 1st lockdown ( $164,604 \pm 47,610$  and  $481,199 \pm 49,858$  in 2020 and 2016–2019, respectively) and 2nd lockdown ( $144,517 \pm 91,765$  and  $493,958 \pm 71,284$  in 2020 and 2016–2019, respectively), indicating the reductions of CO, NO, NO<sub>2</sub>, and BC were mainly attributed to the attenuated traffic density. However, the traffic less contributed to O<sub>3</sub>, PM<sub>10</sub>, and PM<sub>2.5</sub>, which traffic factors were less than 0.05 (Fig. 3). It is because PM<sub>10</sub> and PM<sub>2.5</sub> has complex emission sources and natural generation processes (e.g, dust, heating, nucleation, secondary inorganic aerosol) (Hopke et al., 2022). The unchanged PMs concentrations during lockdown could have relations with the physico-chemical process in the atmosphere locally (Cameletti, 2020) and enhanced PM<sub>2.5</sub> levels were also induced by long-range transportation (Graham et al., 2020). Both anticyclonic weather and long-range transportation contributed to O<sub>3</sub> as well (Pope et al., 2016). In addition, the spatio-temporal of air pollution such as O<sub>3</sub> and PM<sub>10</sub> was also related to the land use characteristics (Yoo et al., 2015). Since the observed air pollution data was collected from different land-use (i.e. urban background, urban traffic, and suburban background) in Augsburg.

It is interesting to observe the role of wind speed and wind direction on PM<sub>10</sub>, PM<sub>2.5</sub>, and BC concentrations, which driving factors were higher than 0.15 and 0.2, respectively. We further showed the distributions of PM<sub>10</sub>, PM<sub>2.5</sub>, and BC with wind speed and wind direction to interpret their interplay in Table 2. The radius graphs represented the wind speed (m/s) and direction (0–360°), while the color represented mass concentrations of air pollutants in Fig. 4. The wind frequencies were predominant in the west (13.08%) and east (10.18%) directions compared to north (5.85%) and south (5.63%) directions. But the PM<sub>10</sub> and PM<sub>2.5</sub> in west ( $18.68$  and  $11.97 \text{ }\mu\text{g/m}^3$ ) and east ( $18.77$  and  $12.04 \text{ }\mu\text{g/m}^3$ ) directions did not show consistent trends to the north ( $18.73$  and  $12.02 \text{ }\mu\text{g/m}^3$ ) and south ( $18.64$  and  $11.94 \text{ }\mu\text{g/m}^3$ ) directions. The average wind speeds in west (2.91 m/s) and south (2.91 m/s) directions were higher than north (2.90 m/s) and east (2.88 m/s) direction. The PM<sub>10</sub> were lower in west ( $18.68 \text{ }\mu\text{g/m}^3$ ) and south ( $18.64 \text{ }\mu\text{g/m}^3$ ) direction than in north ( $18.73 \text{ }\mu\text{g/m}^3$ ) and east direction ( $18.77 \text{ }\mu\text{g/m}^3$ ). This is also similar to PM<sub>2.5</sub>, where the west ( $11.97 \text{ }\mu\text{g/m}^3$ ) and south ( $11.94 \text{ }\mu\text{g/m}^3$ ) direction were lower than north ( $12.02 \text{ }\mu\text{g/m}^3$ ) and east ( $12.04 \text{ }\mu\text{g/m}^3$ ) direction. It indicated that strong wind speeds resulted in low concentrations of PM<sub>10</sub> and PM<sub>2.5</sub>. In contrast, wind direction is more complex to explain which had relations with the land characteristic for each monitoring station. In a previous report, both wind speed and directions showed important effects on detecting ultrafine particle near a highway (Zhu et al., 2002).

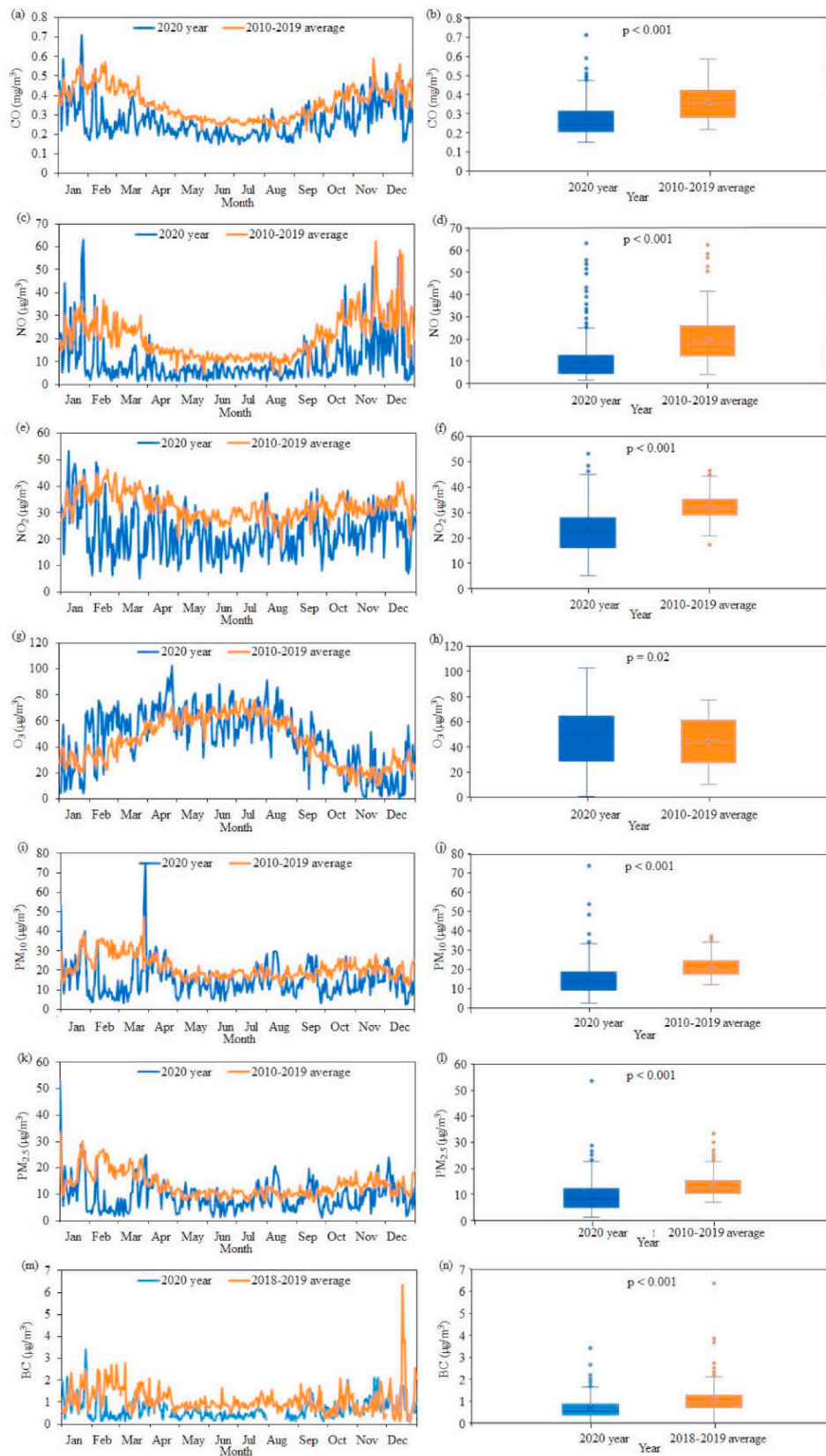


**Fig. 2.** The annual of air pollutants of CO (a, b), NO (c, d), NO<sub>2</sub> (e, f), O<sub>3</sub> (g, h), PM<sub>10</sub> (i, j), PM<sub>2.5</sub> (k, l), and BC (m, n) in Augsburg between 2020 and 2010–2019. The left panel indicated time series of the monthly mean concentrations in the periods studied. The right panel indicated comparison of the total concentrations in the periods studied.

**Table 1**

The fitting effects of four models based on R<sup>2</sup>, MSE, RMSE, MAE, and MAPE values (Random Forest, RF; K-nearest Neighbors, KNN; Linear regression, LN; and Lasso regression, Lasso).

Air pollution	Comparison of different model
CO	RF > LN > Lasso > KN
NO	RF > LN = Lasso > KN
NO <sub>2</sub>	RF > LN = Lasso > KN
O <sub>3</sub>	RF > LN = Lasso > KN
PM <sub>10</sub>	RF > KN > LN = Lasso
PM <sub>2.5</sub>	RF > LN = Lasso > KN
BC	RF > LN = Lasso > KN

3.3. Prediction of air pollutants without lockdown

3.3.1. Changes of CO, NO, NO<sub>2</sub>, and BC

This study used the Random Forest based on air pollutant data, meteorological and traffic data, as well as weekdays and holidays from 2016 to 2019 to predict theoretical pollutant concentration values in two lockdown periods in the absence of lockdown measures and compared them with actual monitoring values (Fig. 5). The actually monitored values for each air pollutant were significantly different from the theoretical predicted values ( $p < 0.001$ ) except NO in 2nd lockdown with p-value of 0.055. Specifically, the theoretical predicted average concentrations of CO, NO, NO<sub>2</sub>, and BC during the 1st lockdown were  $0.33 \pm 0.07 \text{ mg/m}^3$ ,  $13.91 \pm 12.27 \text{ }\mu\text{g/m}^3$ ,  $30.23 \pm 9.02 \text{ }\mu\text{g/m}^3$ , and  $1.29 \pm 0.65 \text{ }\mu\text{g/m}^3$ , which were higher than the actually measured values indicating lockdown played an important role in the reduction of CO, NO, NO<sub>2</sub>, and BC (Table 3). This was mainly due to the measures

during the pandemic situation where the fossil fuel-powered transportation attenuated and the frequency of travel significantly reduced (Fig. S2). The similar results were also reported by previous studies (Collivignarelli et al., 2020; Patel et al., 2020), which highlighted a significant decrease in BC, CO, and NO<sub>2</sub> concentration due to the reduction of traffic density. The similar phenomenon for the reductions of CO, NO<sub>2</sub>, and BC were also found in the 2nd lockdown.

3.3.2. Changes of O<sub>3</sub>

For the 1st lockdown, the actually measured O<sub>3</sub> was  $62.88 \pm 33.65 \text{ }\mu\text{g/m}^3$ , which significantly increased 15.62% compared to the predicted O<sub>3</sub> ( $53.06 \pm 27.70 \text{ }\mu\text{g/m}^3$ ). This was consistent with the results from Munir et al. (2021) who reported the increased O<sub>3</sub> in Berkshire, UK, during the spring lockdown. Liu et al. (2020a) found that lower emissions of NO<sub>x</sub> would weaken the titration effect of NO and result in a larger accumulation of O<sub>3</sub>. This was also supported by Collivignarelli et al. (2020), Dantas et al. (2020), and Tobias et al. (2020) who showed that the increased O<sub>3</sub> during lockdown was probably owing to the

**Table 2**

The distributions of PM<sub>10</sub>, PM<sub>2.5</sub>, BC, wind speed and frequency in different directions based on Augsburg data from August 01, 2016 to September 30, 2019.

Targets	North	East	West	South
Wind frequency (%)	5.85	10.18	13.08	5.63
Wind speed (m/s)	2.90	2.88	2.91	2.91
BC ( $\mu\text{g/m}^3$ )	1.13	1.13	1.13	1.13
PM <sub>2.5</sub> ( $\mu\text{g/m}^3$ )	12.02	12.04	11.97	11.94
PM <sub>10</sub> ( $\mu\text{g/m}^3$ )	18.73	18.77	18.68	18.64

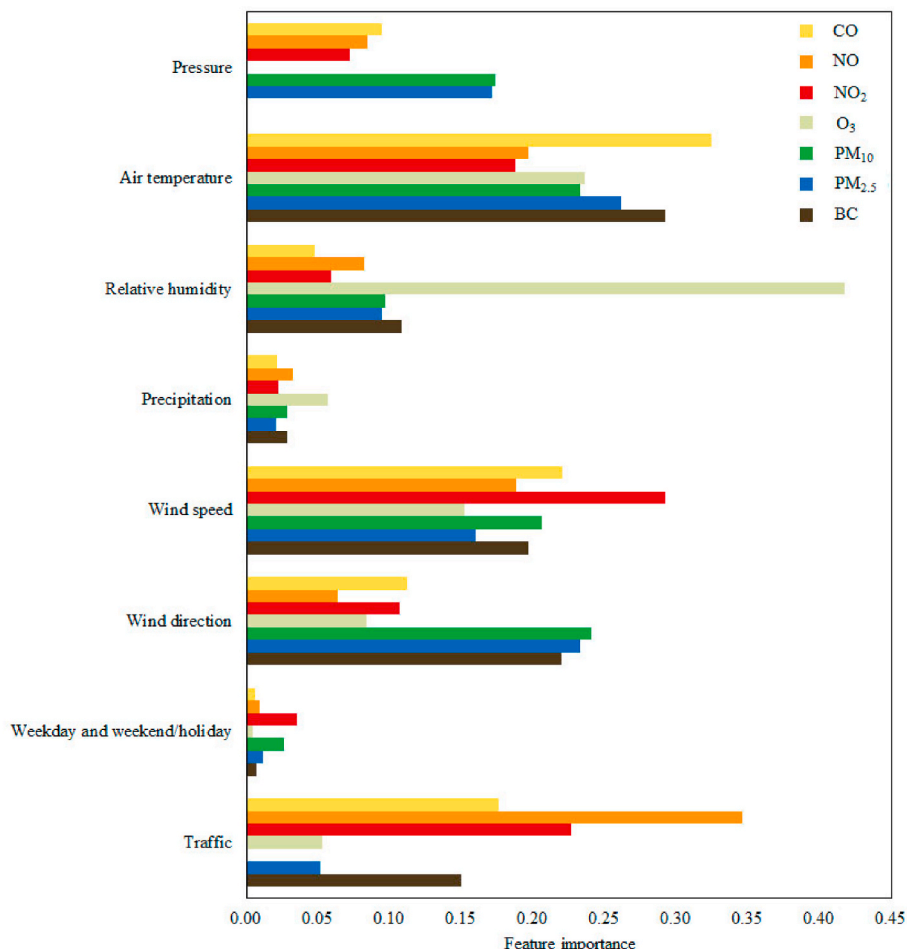


Fig. 3. Driving factor of different variables based on Random Forest data in Augsburg from August 01, 2016 to September 30, 2019.

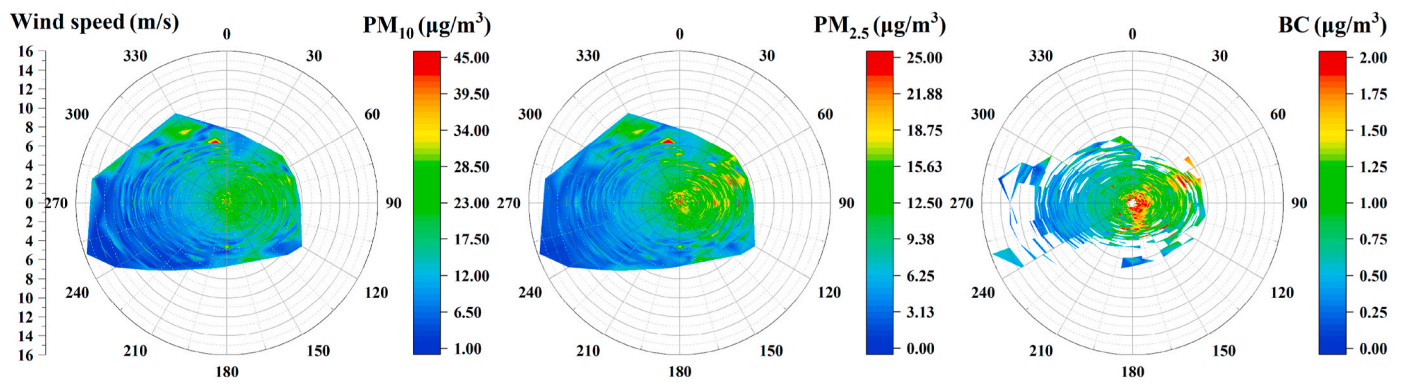


Fig. 4. Relationship of PM<sub>10</sub>, PM<sub>2.5</sub>, and BC with wind direction and wind speed in Augsburg from August 01, 2016 to September 30, 2019.

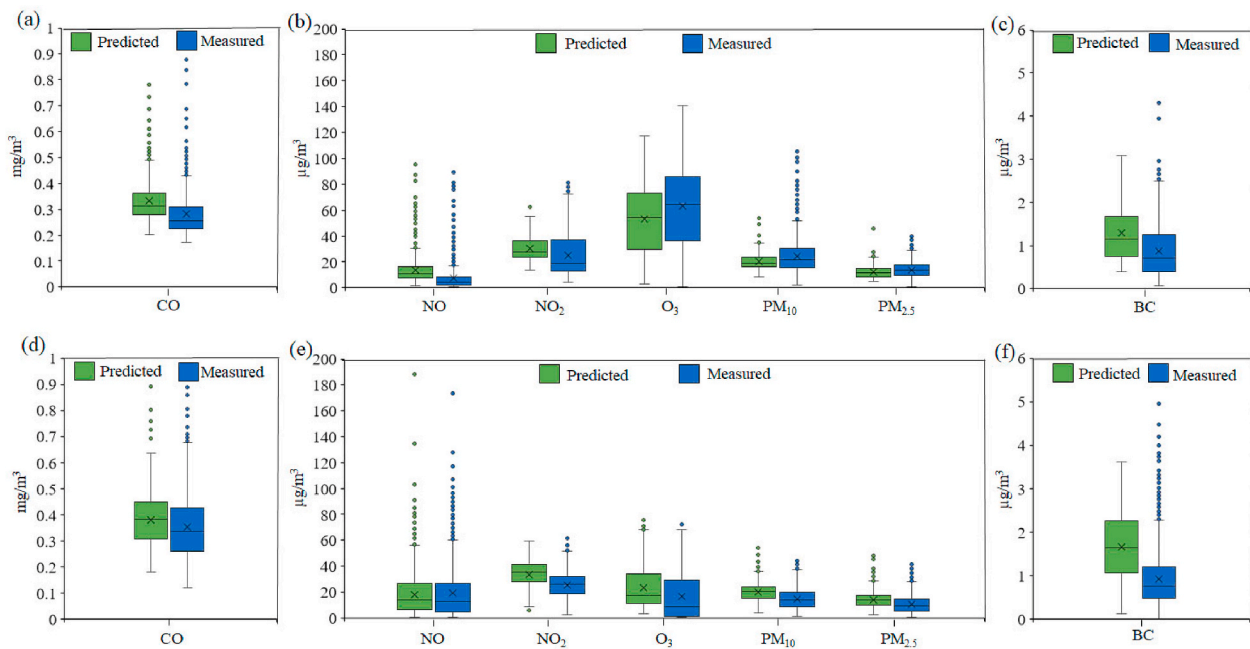


Fig. 5. The predicted and measured values of different air pollutants in the 1st lockdown (a) CO (b) NO, NO<sub>2</sub>, O<sub>3</sub>, PM<sub>10</sub>, PM<sub>2.5</sub>, and (c) BC as well as in the 2nd Lockdown (d) CO (e) NO, NO<sub>2</sub>, O<sub>3</sub>, PM<sub>10</sub>, PM<sub>2.5</sub>, and (f) BC in Augsburg in 2020.

Table 3

The predicted values and measured values during lockdown. (Mean ± SD; Change % = (a measured value – a predicted value)/a measured value · 100%).

Pollutant	16/03–19/04 (1st lockdown)			02/11–31/12 (2nd lockdown)		
	Predicted values	Measured values	Change %	Predicted values	Measured values	Change %
CO (mg/m <sup>3</sup> )	0.33 ± 0.07	0.28 ± 0.09	–18.21	0.38 ± 0.10	0.35 ± 0.13	–7.67
NO (µg/m <sup>3</sup> )	13.91 ± 12.27	7.92 ± 11.55	–75.68	18.17 ± 15.34	19.14 ± 19.55	4.88
NO <sub>2</sub> (µg/m <sup>3</sup> )	30.23 ± 9.02	24.83 ± 16.19	–21.75	33.65 ± 10.31	25.44 ± 10.18	–32.28
O <sub>3</sub> (µg/m <sup>3</sup> )	53.06 ± 27.70	62.88 ± 33.65	15.62	23.45 ± 16.83	16.71 ± 17.99	–40.39
PM <sub>10</sub> (µg/m <sup>3</sup> )	19.99 ± 5.44	24.44 ± 14.58	18.23	19.85 ± 7.05	14.77 ± 8.09	–34.37
PM <sub>2.5</sub> (µg/m <sup>3</sup> )	12.26 ± 4.64	13.63 ± 6.58	10.06	13.83 ± 5.95	10.59 ± 6.92	–30.62
BC (µg/m <sup>3</sup> )	1.29 ± 0.65	0.87 ± 0.60	–48.92	1.65 ± 0.74	0.92 ± 0.69	–79.08

decreased NO in Barcelona (Spain) and Milan (Italy), respectively. In the 2nd lockdown, the measured O<sub>3</sub> (16.71 ± 17.99 µg/m<sup>3</sup>) decreased 40.39% compared to the predicted O<sub>3</sub> (23.45 ± 16.83 µg/m<sup>3</sup>). It could be the weakened photochemistry effects (Qi et al., 2021) in autumn and winter time, which reduced local ozone production.

### 3.3.3. Changes of PM

Similar to O<sub>3</sub>, our study also showed opposite changes of PM<sub>10</sub> and PM<sub>2.5</sub> in two lockdowns. For the 1st lockdown, the actual concentrations

of PM<sub>10</sub> and PM<sub>2.5</sub> were 24.44 ± 14.58 and 13.63 ± 6.58 µg/m<sup>3</sup>, increasing to 18.23% and 10.06%, respectively, compared to the predicted PMs. However, in the 2nd lockdown, the concentrations of PM<sub>10</sub> and PM<sub>2.5</sub> reduced 34.37% and 30.62%, respectively (Table 3). In recent studies (Gu et al., 2021; Liu et al., 2021c), the observed PM<sub>2.5</sub> did not exhibit equivalent changes as the gas precursors during the strict COVID-19 lockdown periods. Thus, different mechanisms other than the primary emission and secondary PM formation changes were suggested to largely contribute to the enhancement of fine particles in Augsburg.



Zangari et al. (2020) also found that the PM<sub>2.5</sub> levels in New York showed no significant difference during lockdown period in 2020 when compared to 2015–2019. However, during the 2nd lockdown, the traffic flow was further reduced compared to the 1st lockdown due to stricter measures to restrict people travel. At the same time, a prohibition on fireworks in public places may lead to a significant reduction especially between Christmas and New Year eve (24/12–31/12), which further reduced the sources of air pollution (Khedr et al., 2022), and thus the concentration of pollutants during the 2nd lockdown was decreased.

### 3.3.4. Comparison of the measured air pollutants between two lockdowns

CO, NO, NO<sub>2</sub>, and BC were lower in the 1st lockdown ( $0.28 \pm 0.09$  mg/m<sup>3</sup>,  $7.92 \pm 11.55$  µg/m<sup>3</sup>,  $24.83 \pm 16.19$  µg/m<sup>3</sup>, and  $0.87 \pm 0.60$  µg/m<sup>3</sup>) than that in the 2nd lockdown ( $0.35 \pm 0.13$  mg/m<sup>3</sup>,  $19.14 \pm 19.55$  µg/m<sup>3</sup>,  $25.44 \pm 10.18$  µg/m<sup>3</sup>, and  $0.92 \pm 0.69$  µg/m<sup>3</sup>) (Table 3). Higher temperature and wind speed in the 1st lockdown ( $7.12 \pm 7.00$  °C and  $2.92 \pm 1.99$  m/s) accelerated these air pollution dispersion than that in the 2nd lockdown ( $2.88 \pm 4.50$  °C and  $2.40 \pm 1.40$  m/s), even the traffic flow was larger in the 1st lockdown (164,604 ± 112,759 per hour) than that in the 2nd lockdown (144,713 ± 140,167 per hour) (Table S8), further indicating temperature and wind speed made a high contribution to the air pollution concentrations. However, O<sub>3</sub>, PM<sub>10</sub>, and PM<sub>2.5</sub> were higher in the 1st lockdown ( $62.88 \pm 33.65$ ,  $24.44 \pm 14.58$ ,  $13.63 \pm 6.58$  µg/m<sup>3</sup>) than that in the 2nd lockdown ( $16.71 \pm 17.99$ ,  $14.77 \pm 8.09$ ,  $10.59 \pm 6.92$  µg/m<sup>3</sup>) (Table 3). The warm temperature, prolonged sunlight, low relative humidity, and decreased NO greatly contributed to the extraordinary high O<sub>3</sub> in the 1st lockdown (Table S8). The higher PMs in the 1st lockdown could attribute to the physico-chemical process in the atmosphere. In this condition, the higher pressure and temperature in the 1st lockdown could benefit this process than that in the 2nd lockdown.

## 4. Conclusions

In this study, we compared the annual levels of air pollutants in 2020 to the record data in 2010–2019 in Augsburg. The air quality (CO, NO, NO<sub>2</sub>, PM<sub>10</sub>, PM<sub>2.5</sub>, and BC) was significantly improved in 2020, which was because of restriction measures during pandemic situation. In a deep study to simulate and predict air pollutants, we used four modes (Random Forest, K-nearest Neighbors, Linear regression, and Lasso Regression) based on meteorological data, traffic density, weekday and weekend/holiday. Random Forest showed the best fitting performance and was used to predict air pollutants during lockdown periods. It turned out that temperature and wind speed were the two most important factors for all air pollutants predictions. Traffic factor was very important in the predictions of CO, NO, NO<sub>2</sub> and BC but not for O<sub>3</sub>, PM<sub>10</sub>, and PM<sub>2.5</sub> indicating the necessity to include traffic variable for these air pollutants model simulation. It was interesting to observe the role of wind directions on BC, PM<sub>10</sub> and PM<sub>2.5</sub> predictions but its functions were more complex to explain which were associated with the used land characteristic. VOCs factor could be considered in the future O<sub>3</sub> prediction to achieve the more accuracy results. The measured CO, NO, NO<sub>2</sub>, and BC were significantly decreased compared to the predicted values during lockdowns which were owing to the limitation of traffic and industrial activities. The measured O<sub>3</sub> and PMS significantly increased in 1st lockdown period even with restriction measures, which could be owing to their complex physico-chemical formation in atmosphere. This study presented a certain degree of idea to the regulatory bodies on planning and implementation of strict air quality control plans and emission control strategies to improve environmental and human health. Overall, this analysis of air quality data shows that the strict implementation of lockdown measures in Augsburg during COVID-19 (and associated reductions in transport) contributed to the improvement of local air quality and the necessity to include important variables for the simulations and predictions of air pollution.

## Credit author statement

**Xin Cao:** Data curation, Methodology, Software, Writing original draft. **Xiansheng Liu:** Methodology, Software, Writing original draft, Supervision. **Hadiatullah Hadiatullah:** Data curation, Methodology, Writing review & editing. **Yanning Xu:** Methodology. **Xun Zhang:** Software. **Jan Bendl:** Data curation. **Josef Cyrus:** Data curation. **Ralf Zimmerman:** Writing review & editing. **Thomas Adama:** Investigation.

## Declaration of competing interest

The authors declare that they have no known competing financial interests or personal relationships that could have appeared to influence the work reported in this paper.

## Acknowledgements

The work is funded by National Natural Science Foundation of China (42101470), Support Project of High-level Teachers in Beijing Municipal Universities in the Period of 13th Five-year Plan (CIT&TCD201904037), the Germany Federal Ministry of Transport and Digital Infrastructure (BMVI) as part of SmartAQnet (19F2003B), the dtcc.bw -Digitalization and Technology Research Center of the Bundeswehr (project MORE). We would like to thank to the Administration of Augsburg City for giving access to the traffic data (Tiefbauamt, Markus Furnier).

## Appendix A. Supplementary data

Supplementary data to this article can be found online at <https://doi.org/10.1016/j.apr.2022.101536>.

## References

- Abou El-Magd, I., Zanaty, N., 2021. Impacts of short-term lockdown during COVID-19 on air quality in Egypt. *Egyptian Journal of Remote Sensing and Space Science* 24, 493–500. <https://doi.org/10.1016/j.ejrs.2020.10.003>.
- Adame, J.A., Hernández-Ceballos, M.Á., Sorribas, M., Lozano, A., de la Morena, B.A., 2014. Weekend-weekday effect assessment for O<sub>3</sub>, NO<sub>x</sub>, CO and PM<sub>10</sub> in Andalusia, Spain (2003–2008). *Aerosol Air Qual. Res.* 14, 1862–1874. <https://doi.org/10.4209/aaqr.2014.02.0026>.
- Aini, N., Mustafa, M.S., 2020, October. Data mining approach to predict air pollution in Makassar. In: 2020 2nd International Conference on Cybernetics and Intelligent System (ICORIS). IEEE, pp. 1–5. <https://doi.org/10.1109/ICORIS50180.2020.9320800>.
- Araujo, J.A., 2011. Particulate air pollution, systemic oxidative stress, inflammation, and atherosclerosis. *Air Quality, Atmosphere and Health* 4, 79–93. <https://doi.org/10.1007/s11869-010-0101-8>.
- Arif, M., Parveen, S., 2021. Carcinogenic effects of indoor black carbon and particulate matters (PM<sub>2.5</sub> and PM<sub>10</sub>) in rural households of India. *Environ. Sci. Pollut. Control Ser.* 28, 2082–2096. <https://doi.org/10.1007/s11356-020-10668-5>.
- Balamurugan, V., Chen, J., Qu, Z., Bi, X., Gensheimer, J., Shekhar, A., Bhattacharjee, S., Keutsch, F.N., 2021. Tropospheric NO<sub>2</sub> and O<sub>3</sub> response to COVID-19 lockdown restrictions at the national and urban scales in Germany. *J. Geophys. Res. Atmos.* 126. <https://doi.org/10.1029/2021JD035440>.
- Balmes, J.R., Arjomandi, M., Bromberg, P.A., Costantini, M.G., Dagincourt, N., Hazucha, M.J., Hollenbeck-Pringle, D., Rich, D.Q., Stark, P., Frampton, M.W., 2019. Ozone effects on blood biomarkers of systemic inflammation, oxidative stress, endothelial function, and thrombosis: the multicenter ozone study in older subjects (MOSES). *PLoS One* 14. <https://doi.org/10.1371/journal.pone.0222601>.
- Begam, G.R., Vachaspati, C.V., Ahammed, Y.N., Kumar, K.R., Babu, S.S., Reddy, R.R., 2016. Measurement and analysis of black carbon aerosols over a tropical semi-arid station in Kadapa, India. *Atmos. Res.* 171, 77–91. <https://doi.org/10.1016/j.atmosres.2015.12.014>.
- Bera, B., Bhattacharjee, S., Sengupta, N., Saha, S., 2021. PM<sub>2.5</sub> concentration prediction during COVID-19 lockdown over Kolkata metropolitan city, India using MLR and ANN models. *Environmental Challenges* 4, 100155. <https://doi.org/10.1016/j.envc.2021.100155>.
- Briz-Redón, Á., Belenguer-Sapiña, C., Serrano-Aroca, Á., 2021. Changes in air pollution during COVID-19 lockdown in Spain: a multi-city study. *J. Environ. Sci. (China)* 101, 16–26. <https://doi.org/10.1016/j.jes.2020.07.029>.
- Burns, J., Hoffmann, S., Kurz, C., Laxy, M., Polus, S., Rehfuess, E., 2021. COVID-19 mitigation measures and nitrogen dioxide – a quasi-experimental study of air quality in Munich, Germany. *Atmos. Environ.* 246, 118089. <https://doi.org/10.1016/j.atmosenv.2020.118089>.

- Cameletti, M., 2020. The effect of corona virus lockdown on air pollution: evidence from the city of brescia in lombardia region (Italy). *Atmos. Environ.* 239, 117794 <https://doi.org/10.1016/j.atmosenv.2020.117794>.
- Cazorla, M., Herrera, E., Palomeque, E., Saud, N., 2021. What the COVID-19 lockdown revealed about photochemistry and ozone production in Quito, Ecuador. *Atmos. Pollut. Res.* 12, 124–133. <https://doi.org/10.1016/j.apr.2020.08.028>.
- Chen, Z.H., Cheng, S.Y., Li, J.B., Guo, X.R., Wang, W.H., Chen, D.S., 2008. Relationship between atmospheric pollution processes and synoptic pressure patterns in northern China. *Atmos. Environ.* 42, 6078–6087. <https://doi.org/10.1016/j.atmosenv.2008.03.043>.
- Collivignarelli, M.C., Abbà, A., Bertanza, G., Pedrazzani, R., Ricciardi, P., Carnevale Miino, M., 2020. Lockdown for CoVid-2019 in Milan: what are the effects on air quality? *Sci. Total Environ.* 732, 139280 <https://doi.org/10.1016/j.scitotenv.2020.139280>.
- Dantas, G., Siciliano, B., França, B.B., da Silva, C.M., Arbilla, G., 2020. The impact of COVID-19 partial lockdown on the air quality of the city of Rio de Janeiro, Brazil. *Sci. Total Environ.* 729, 139085 <https://doi.org/10.1016/j.scitotenv.2020.139085>.
- Das, M., Das, A., Sarkar, R., Saha, S., Mandal, P., 2021. Regional scenario of air pollution in lockdown due to COVID-19 pandemic: evidence from major urban agglomerations of India. *Urban Clim.* 37, 100821 <https://doi.org/10.1016/j.uclim.2021.100821>.
- Farias, F., ApSimon, H., 2006. Relative contributions from traffic and aircraft NOx emissions to exposure in West London. *Environ. Model. Software* 21, 477–485. <https://doi.org/10.1016/j.envsoft.2004.07.010>.
- Gariazzo, C., Carlino, G., Silibello, C., Renzi, M., Finardi, S., Pepe, N., et al., 2020. A multi-city air pollution population exposure study: combined use of chemical-transport and random-forest models with dynamic population data. *Sci. Total Environ.* 724, 138102 <https://doi.org/10.1016/j.scitotenv.2020.138102>.
- Gu, Y., Yan, F., Xu, J., Duan, Y., Fu, Q., Qu, Y., Liao, H., 2021. Mitigated PM2.5 changes by the regional transport during the COVID-19 lockdown in Shanghai, China. *Geophys. Res. Lett.* 48 <https://doi.org/10.1029/2021GL092395>.
- Graham, A.M., Pringle, K.J., Arnold, S.R., Pope, J.R., Vieno, M., Butt, E.W., Conibear, L., Stirling, E.L., McQuaid, J.B., 2020. Impact of weather types on UK ambient particulate matter concentrations. *Atmos. Environ.* X 5, 100061. <https://doi.org/10.1016/j.aeaoa.2019.100061>.
- Gualtieri, G., Brilli, L., Carotenuto, F., Vagnoli, C., Zaldei, A., Gioli, B., 2020. Quantifying road traffic impact on air quality in urban areas: a Covid19-induced lockdown analysis in Italy. *Environ. Pollut.* 267, 115682 <https://doi.org/10.1016/j.envpol.2020.115682>.
- Hopke, P.K., Feng, Y., Dai, Q., 2022. Source apportionment of particle number concentrations: a global review. *Sci. Total Environ.* 819, 153104 <https://doi.org/10.1016/j.scitotenv.2022.153104>.
- Hu, B., Guo, H., Zhou, P., Shi, Z.L., 2021. Characteristics of SARS-CoV-2 and COVID-19. *Nat. Rev. Microbiol.* 19, 141–154. <https://doi.org/10.1038/s41579-020-00459-7>.
- Jayaweera, M., Perera, H., Gunawardana, B., Manatunge, J., 2020. Transmission of COVID-19 virus by droplets and aerosols: a critical review on the unresolved dichotomy. *Environ. Res.* 188, 109819 <https://doi.org/10.1016/j.envres.2020.109819>.
- Khedr, M., Liu, X., Hadiatullah, H., Orasche, J., Zhang, X., Cyrus, J., Michalke, B., Zimmermann, R., Schnelle-Kreis, J., 2022. Influence of New Year's fireworks on air quality – a case study from 2010 to 2021 in Augsburg, Germany. *Atmos. Pollut. Res.* 13, 101341 <https://doi.org/10.1016/j.apr.2022.101341>.
- Kim, K.H., Jahan, S.A., Kabir, E., 2013. A review on human health perspective of air pollution with respect to allergies and asthma. *Environ. Int.* 59, 41–52. <https://doi.org/10.1016/j.envint.2013.05.007>.
- Kim, S.Y., Kim, E., Kim, W.J., 2020. Health effects of ozone on respiratory diseases. *Tuberc. Respir. Dis.* 83 <https://doi.org/10.4046/TRD.2020.0154>. S6–S11.
- Krecl, P., Cipoli, Y.A., Targino, A.C., Castro, L.B., Gidhagen, L., Malucelli, F., Wolf, A., 2020. Cyclists' exposure to air pollution under different traffic management strategies. *Sci. Total Environ.* 723, 138043 <https://doi.org/10.1016/j.scitotenv.2020.138043>.
- Kumari, P., Toshniwal, D., 2020. Impact of lockdown on air quality over major cities across the globe during COVID-19 pandemic. *Urban Clim.* 34, 100719 <https://doi.org/10.1016/j.uclim.2020.100719>.
- Lawal, A.O., 2017. Air particulate matter induced oxidative stress and inflammation in cardiovascular disease and atherosclerosis: the role of Nrf 2 and AhR-mediated pathways. *Toxicol. Lett.* 270, 88–95. <https://doi.org/10.1016/j.toxlet.2017.01.017>.
- Li, R., Cui, L., Li, J., Zhao, A., Fu, H., Wu, Y., Zhang, L., Kong, L., Chen, J., 2017. Spatial and temporal variation of particulate matter and gaseous pollutants in China during 2014–2016. *Atmos. Environ.* 161, 235–246. <https://doi.org/10.1016/j.atmosenv.2017.05.008>.
- Liu, T., Wang, X., Hu, J., Wang, Q., An, J., Gong, K., Sun, J., Li, L., Qin, M., Li, J., Tian, J., Huang, Y., Liao, H., Zhou, M., Hu, Q., Yang, R., Wang, H., Huang, C., 2020a. Driving forces of changes in air quality during the COVID-19 lockdown period in the yangtze river delta region, China. *Environ. Sci. Technol. Lett.* 7, 779–786. <https://doi.org/10.1021/acs.estlett.0c00511>.
- Liu, X., Schnelle-Kreis, J., Zhang, X., Bendl, J., Khedr, M., Jakobi, G., Schloter-Hai, B., Hovorka, J., Zimmermann, R., 2020b. Integration of air pollution data collected by mobile measurement to derive a preliminary spatiotemporal air pollution profile from two neighboring German-Czech border villages. *Sci. Total Environ.* 722, 137632 <https://doi.org/10.1016/j.scitotenv.2020.137632>.
- Liu, X., Hadiatullah, H., Zhang, X., Hill, L.D., White, A.H.A., Schnelle-Kreis, J., Bendl, J., Jakobi, G., Schloter-Hai, B., Zimmermann, R., 2021a. Analysis of mobile monitoring data from the microAeth® MA200 for measuring changes in black carbon on the roadside in Augsburg. *Atmos. Meas. Tech.* 14, 5139–5151. <https://doi.org/10.5194/amt-14-5139-2021>.
- Liu, X., Hadiatullah, H., Tai, P., Xu, Y., Zhang, X., Schnelle-Kreis, J., Schloter-Hai, B., Zimmermann, R., 2021b. Air pollution in Germany: spatio-temporal variations and their driving factors based on continuous data from 2008 to 2018. *Environ. Pollut.* 276, 116732 <https://doi.org/10.1016/j.envpol.2021.116732>.
- Liu, X., Zhang, X., Schnelle-Kreis, J., Jakobi, G., Cao, X., Cyrus, J., Yang, L., Schloter-Hai, B., Abbaszade, G., Orasche, J., Khedr, M., Kowalski, M., Hank, M., Zimmermann, R., 2021c. Spatiotemporal characteristics and driving factors of black carbon in Augsburg, Germany: combination of mobile monitoring and street view images. *Environ. Sci. Technol.* 55, 160–168. <https://doi.org/10.1021/acs.est.0c04776>.
- Munir, S., Luo, Z., Dixon, T., 2021. Comparing different approaches for assessing the impact of COVID-19 lockdown on urban air quality in Reading, UK. *Atmos. Res.* 261, 105730 <https://doi.org/10.1016/j.atmosres.2021.105730>.
- Patel, H., Talbot, N., Salmund, J., Dirks, K., Xie, S., Davy, P., 2020. Implications for air quality management of changes in air quality during lockdown in Auckland (New Zealand) in response to the 2020 SARS-CoV-2 epidemic. *Sci. Total Environ.* 746, 141129 <https://doi.org/10.1016/j.scitotenv.2020.141129>.
- Pitz, M., Birmili, W., Schmid, O., Peters, A., Wichmann, H.E., Cyrus, J., 2008. Quality control and quality assurance for particle size distribution measurements at an urban monitoring station in Augsburg, Germany. *J. Environ. Monit.* 10, 1017–1024. <https://doi.org/10.1039/b807264g>.
- Pope, R.J., Butt, E.W., Chipperfield, M.P., Doherty, R.M., Fenech, S., Schmidt, A., Arnold, S.R., Savage, N.H., 2016. The impacts of synoptic weather on UK surface ozone and implications for premature mortality. *Environ. Res. Lett.* 11, 124004. <https://doi.org/10.1088/1748-9326/11/12/124004>.
- Qi, J., Mo, Z., Yuan, B., Huang, S., Huangfu, Y., Wang, Z., Li, X., Yang, S., Wang, Wenjie, Zhao, Y., Wang, X., Wang, Weiwen, Liu, K., Shao, M., 2021. An observation approach in evaluation of ozone production to precursor changes during the COVID-19 lockdown. *Atmos. Environ.* 262, 118618 <https://doi.org/10.1016/j.atmosenv.2021.118618>.
- Sethi, J.K., Mittal, M., 2021. An efficient correlation based adaptive LASSO regression method for air quality index prediction. *Earth Science Informatics* 14 (4), 1777–1786. <https://doi.org/10.1007/s12145-021-00618-1>.
- Shen, L., Li, L., Lü, S., Zhang, X., Liu, J., An, J., Zhang, G., Wu, B., Wang, F., 2015. Characteristics of black carbon aerosol in Jiaxing, China during autumn 2013. *Particulology* 20, 10–15. <https://doi.org/10.1016/j.partic.2014.08.002>.
- Sicard, P., de Marco, A., Agathokleous, E., Feng, Z., Xu, X., Paoletti, E., Rodriguez, J.J.D., Calatayud, V., 2020. Amplified ozone pollution in cities during the COVID-19 lockdown. *Sci. Total Environ.* 735, 139542 <https://doi.org/10.1016/j.scitotenv.2020.139542>.
- Szyszkowicz, M., Rowe, B.H., 2016. Respiratory health conditions and ambient ozone: a case-crossover study. *Insights in Chest Diseases* 1, 1–9.
- Tobías, A., Carnerer, C., Reche, C., Massagué, J., Via, M., Minguillón, M.C., Alastuey, A., Querol, X., 2020. Changes in air quality during the lockdown in Barcelona (Spain) one month into the SARS-CoV-2 epidemic. *Sci. Total Environ.* 726, 138540 <https://doi.org/10.1016/j.scitotenv.2020.138540>.
- Wang, F., Chen, D.S., Cheng, S.Y., Li, J.B., Li, M.J., Ren, Z.H., 2010. Identification of regional atmospheric PM10 transport pathways using HYSPLIT, MM5-CMAQ and synoptic pressure pattern analysis. *Environ. Model. Software* 25, 927–934. <https://doi.org/10.1016/j.envsoft.2010.02.004>.
- Wang, S., Zhang, Y., Ma, J., Zhu, S., Shen, J., Wang, P., Zhang, H., 2021. Response of decline in air pollution and recovery associated with COVID-19 lockdown in the Pearl River Delta. *Sci. Total Environ.* 756, 143868 <https://doi.org/10.1016/j.scitotenv.2020.143868>.
- World Health Organization. Regional office for Europe. (2003). Health Aspects of Air Pollution with Particulate Matter, Ozone and Nitrogen Dioxide: Report on a WHO Working Group, Bonn, Germany 13-15 January 2003. Copenhagen: WHO Regional Office for Europe. <https://apps.who.int/iris/handle/10665/107478>, 2003.
- Xu, K., Cui, K., Young, L.H., Wang, Y.F., Hsieh, Y.K., Wan, S., Zhang, J., 2020. Air quality index, indicator air pollutants and impact of covid-19 event on the air quality near central China. *Aerosol Air Qual. Res.* 20, 1204–1221. <https://doi.org/10.4209/aaqr.2020.04.0139>.
- Xu, W., Wu, Q., Liu, X., Tang, A., Dore, A.J., Heal, M.R., 2016. Characteristics of ammonia, acid gases, and PM2.5 for three typical land-use types in the North China Plain. *Environ. Sci. Pollut. Control Ser.* 23, 1158–1172. <https://doi.org/10.1007/s11356-015-5648-3>.
- Yoo, J.M., Jeong, M.J., Kim, D., Stockwell, W.R., Yang, J.H., Shin, H.W., Lee, M.I., Song, C.K., Lee, S.D., 2015. Spatiotemporal variations of air pollutants (O3, NO2, SO2, CO, PM10, and VOCs) with land-use types. *Atmos. Chem. Phys.* 15, 10857–10885. <https://doi.org/10.5194/acp-15-10857-2015>.
- Yuchi, W., Gombojav, E., Boldbaatar, B., Galsuren, J., Enkhmaa, S., Beejin, B., et al., 2019. Evaluation of random forest regression and multiple linear regression for predicting indoor fine particulate matter concentrations in a highly polluted city. *Environ. Pollut.* 245, 746–753. <https://doi.org/10.1016/j.envpol.2018.11.034>.
- Zangari, S., Hill, D.T., Charette, A.T., Mirowsky, J.E., 2020. Air quality changes in New York City during the COVID-19 pandemic. *Sci. Total Environ.* 742, 140496 <https://doi.org/10.1016/j.scitotenv.2020.140496>.
- Zhang, L., Cheng, Y., Zhang, Y., He, Y., Gu, Z., Yu, C., 2017. Impact of air humidity fluctuation on the rise of PM mass concentration based on the high-resolution monitoring data. *Aerosol Air Qual. Res.* 17, 543–552. <https://doi.org/10.4209/aaqr.2016.07.0296>.
- Zhang, Q., Streets, D.G., Carmichael, G.R., He, K.B., Huo, H., Kannari, A., Klimont, Z., Park, I.S., Reddy, S., Fu, J.S., Chen, D., Duan, L., Lei, Y., Wang, L.T., Yao, Z.L., 2009.

- Asian emissions in 2006 for the NASA INTEX-B mission. *Atmos. Chem. Phys.* 9, 5131–5153.
- Zhang, Z., Wang, J., Hart, J.E., Laden, F., Zhao, C., Li, T., Zheng, P., Li, D., Ye, Z., Chen, K., 2018. National scale spatiotemporal land-use regression model for PM<sub>2.5</sub>, PM<sub>10</sub> and NO<sub>2</sub> concentration in China. *Atmos. Environ.* 192, 48–54. <https://doi.org/10.1016/j.atmosenv.2018.08.046>.
- Zhu, Y., Hinds, W.C., Kim, S., Sioutas, C., 2002. Concentration and size distribution of ultrafine particles near a major highway. *J. Air Waste Manag. Assoc.* 52, 1032–1042. <https://doi.org/10.1080/10473289.2002.10470842>.